Journal of Harbin Engineering University
ISSN: 1006-7043

Vol 46 No. 4
April 2025

Dual Notched Multilayer Broadside Coupled Ultra-Wideband Bandpass Filter with Folded Meander Slots

***Richard Patience Shema[1], Dominic B. O. Konditi[2], and Elijah Mwangi[3]**

[1]Department of Electrical Engineering, Pan African University Institute for basic Sciences, Technology and Innovation (PAUSTI), hosted within Jomo Kenyatta University of Agriculture and Technology (JKUAT), Nairobi, Kenya

[2]School of Electrical and Electronic Engineering, Technical University of Kenya, Nairobi, Kenya

[3]Department of Electrical and Information Engineering, University of Nairobi, Nairobi, Kenya

*corresponding author: Richard Patience Shema (e-mail: patience.richard@students.jkuat.ac.ke)

Abstract

This paper presents a dual-notched multilayer broadside-coupled ultra-wideband (UWB) bandpass filter with folded meander slots, designed for efficient interference mitigation in UWB systems using multilayer printed circuit board (MPCB) technology. The filter employed a microstrip-coplanar waveguide (CPW) architecture with half-wavelength stepped impedance resonators (SIR) on the upper and lower layers connected vertically via a CPW-rectangular patch resonator on the central layer. The UWB performance is achieved through tight coupling, whereas folded meander slots at the input and output patches create dual notched bands to eliminate interference from narrowband systems, allowing precise frequency adjustment. High-frequency simulations and parametric analyses optimized the filter's dimensions and notch placements, achieving a 96.5% 3 dB fractional bandwidth across the UWB spectrum, with sharply notched bands at 6.0 GHz and 7.6 GHz, attenuated by 19.89 dB and 19.51 dB, respectively, eliminating WLAN and X-band satellite signals. Experimental tests on the RT/Duroid 5880 substrates confirmed the simulated data, validating the minimal insertion loss, enhanced selectivity, and compact design configuration. This study offers a robust solution for interference reduction with significant potential for use in existing UWB wireless communication networks.

Keywords: Bandpass Filter (BPF), dual-notched bands, folded meander slots, multilayer printed circuit board (MPCB), ultra-wideband (UWB)

1. Introduction

Ultra-wideband (UWB) technology has emerged as an essential component for high-speed wireless communication, radar systems, and short-range sensing owing to its capacity to operate over a broad spectrum, typically from 3.1 GHz to 10.6 GHz [1]. However, the cohabitation of UWB systems with narrowband communication technologies, such as worldwide interoperability for microwave access (WiMAX), wireless local area networks (WLAN), and C-band and X-band satellite signals, typically leads to signal interference, which severely affects the performance and reliability of UWB networks. Bandpass filters (BPFs) are key components in UWB systems that assist in preserving the signal integrity by passing the required frequencies while rejecting out-of-band interference.

In the last few decades, researchers have begun to explore multilayer filter technologies that leverage the advantages of miniaturization and improved performance. Three main technologies are widely used: liquid crystal polymers (LCP), low-temperature co-fired ceramics (LTCC), and multilayer printed circuit boards (MPCB). In [2]–[6], the LCP technology was employed to design bandpass filters. However, this technology is expensive, complex, and limited in availability. In [7]–[11], LTCC was used, but it also has a higher processing cost and a complex manufacturing process. In [12]–[17], multilayer PCBs were employed, and they have the advantages of being cost effective and providing more flexibility in component placement, which is the main reason why they were chosen for this project.

In recent years, substantial research has focused on producing compact, high-performance UWB bandpass filters that can decrease interference by introducing notched bands [18]–[21]. A previous study [18] presented an extremely compact UWB multilayered bandpass filter utilizing broadside-coupled striplines with an adjustable notched band. However, this design exhibited suboptimal transmission coefficients within the passband. Another study [19] developed a multilayer bandpass filter featuring a notch created by linking three units in series. However, the resulting notch was excessively broad, making it unsuitable for

the precise suppression of specific interfering frequencies. Furthermore, the designs in [18] and [19] lack the capability of achieving multiple notched bands. A previous study [20] presented a multilayered bandpass filter utilizing multilayer ring resonators, and introduced three techniques for creating notches. However, none of these methods could produce multiple notches with satisfactory transmission coefficients. Another study [21] proposed three filter types based on a multilayer structure of microstrip slot wire microstrip wide-edge coupling, which achieved broadband performance, but lacked the capability to suppress multiple bands. Despite extensive research, the challenge of precisely controlling the notched frequencies while maintaining a compact and efficient design remains.

This study addresses this challenge by proposing a novel dual-notched multilayer broadside-coupled ultra-wideband (UWB) bandpass filter that incorporates folded meander slots. The compact design is achieved through broadside coupling in a multilayer configuration, whereas the folded meander slots enable the precise adjustment of the notched bands. This study aims to enhance the interference rejection in UWB systems while maintaining high selectivity and good transmission coefficients. By combining these strategies, the proposed filter demonstrates an improved performance, contributing to the ongoing development of more effective UWB communication systems.

2. Bandpass Filter Design

2.1. Fundamental Bandpass Filter

The fundamental bandpass filter consists of a single-order wide-side coupling multilayer structure, as illustrated in Fig. 1. This structure is comprised of two dielectric layers and three metal layers.

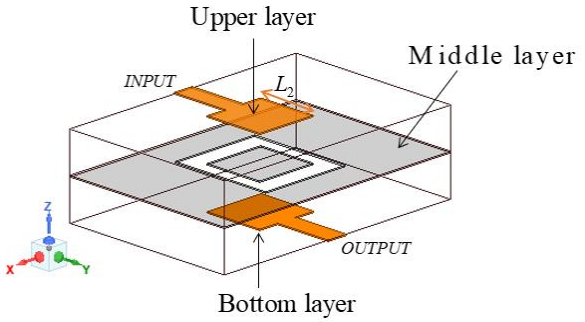

Figure 1. Three-dimensional structure of the fundamental bandpass filter.

The uppermost and lowermost layers of the coupling structure feature identical rectangular microstrip patches that facilitate wide-side vertical coupling through a rectangular slot etched on the ground surface of the middle layer. A rectangular patch of the same size remained in the center of the middle layer to enhance the coupling and provide structural stability to the circuit.

The design is presumed to have coupling of C between the upper and lower patches. Using odd and even-mode analyses of the structure, and assuming perfect matching at the input and output ports, the input port's reflection coefficient (S11) and the insertion loss between the input and output ports (S21) can be calculated as outlined in [22].

$$S_{11} = \frac{1 - C^2\left(1 + \sin^2\left(\beta_{eff} L_2\right)\right)}{\left[\sqrt{1-C^2}\cos\left(\beta_{eff} L_2\right) + j\sin\left(\beta_{eff} L_2\right)\right]^2} \quad (1)$$

$$S_{21} = \frac{j2C\sqrt{1-C^2}\sin\left(\beta_{eff} L_2\right)}{\left[\sqrt{1-C^2}\cos\left(\beta_{eff} L_2\right) + j\sin\left(\beta_{eff} L_2\right)\right]^2} \quad (2)$$

L_2 represents the actual length of the coupled structure, and β_{eff} denotes the effective phase constant within the medium of the coupled structure. For all subsequent calculations, the length L_2 was selected to ensure that $\beta_{eff} = \pi/2$ at the central frequency of the passband of 6.85 GHz.

The filter group delay (τ) is derived from the phase of the insertion loss, and can be determined using the following equation:

$$\tau = \frac{2L_2\sqrt{\varepsilon_r}}{\upsilon\sqrt{1-C^2}}\left[\frac{\cos\left(\arctan\left(\tan\left(\beta_{eff} L_2\right)/\sqrt{1-C^2}\right)\right)}{\cos\left(\beta_{eff} L_2\right)}\right] \quad (3)$$

In this context, υ represents the speed of light in vacuum, and εr denotes the dielectric constant of the substrate.

The transmission coefficient shown in Fig. 2 exhibits a poor performance outside the passband; the upper stopband (11.6GHz to 16GHz) has 5 dB S_{21} attenuation, even if it has a flat group delay of 0.15 ns; the filter is not

qualified to be used in UWB systems. Implementing multiple sections of the broadside coupled structure shown in Fig. 1 is essential to improve the sharpness of the insertion loss drop in the stopband areas below 3.1 GHz and above 10.6 GHz.

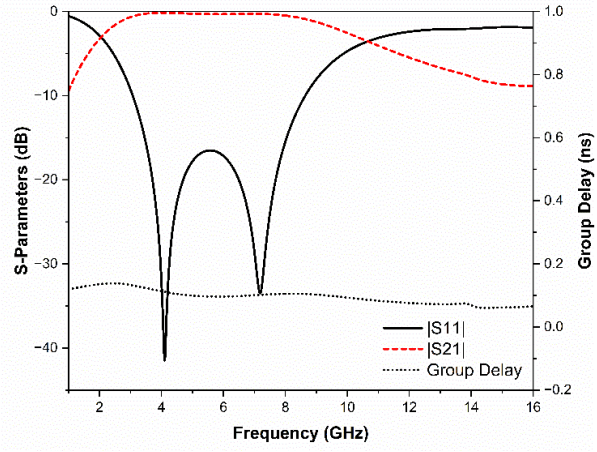

Figure 2. Simulation results of the fundamental filter.

2.2. Ultra-Wideband Bandpass Filter with Improved out of Band Performance

To enhance the performance of both the lower and upper stopbands, while achieving a compact design, three sections of the structure were selected, as illustrated in Fig. 3.

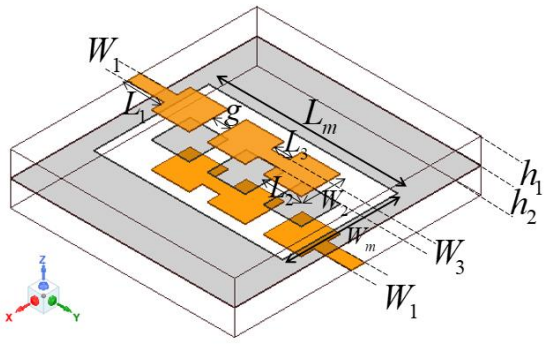

Figure 3. Three dimensional structure of the three sections broadside coupled bandpass filter.

The structural design of the device consists of a three-class cascade wide-side coupling arrangement on the upper and lower layers, with the middle layer featuring a large rectangular slot containing three small rectangular patches aligned with those on the upper and bottom layers. In the cascade region of the ultra-wideband (UWB) filter circuit's top and bottom microstrip structures, a rectangular microstrip patch linked by a 50 Ω microstrip line creates a half-wavelength stepped impedance resonator (SIR). The open-circuit microstrip lines at both ends have length L_2, width W_2, characteristic impedance Z_2, and electrical length θ_2. The central high-impedance microstrip line has a length L_3, width W_3, characteristic impedance Z_3, and electrical length θ_3. The half-wavelength SIR impedance ratio K and the electrical length ratio α are defined as follows [21]:

$$K = Z_2/Z_3 = \tan\theta_2 \tan\theta_3 \quad (4)$$

$$\alpha = \theta_2/(\theta_2+\theta_3) \quad (5)$$

The resonance performance of the circuit is significantly influenced by two key parameters: impedance ratio K and electrical length ratio α. In addition, the passband width is significantly affected by the dimensions of the rectangular slot at the mid-layer, specifically, its width Wm and length L_m [21].

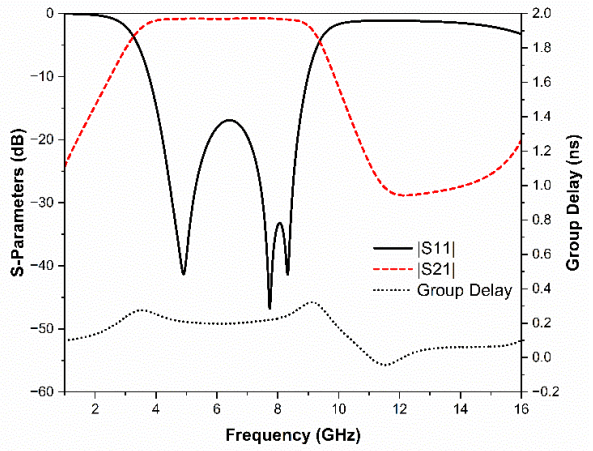

Figure 4. Simulation results of the three-section multilayer bandpass filter.

The out-of-band performance was improved, as demonstrated in Fig. 4; the upper stopband from 10.67 GHz to 16 GHz was obtained with better than 20 dB attenuation. The filter has a 3 dB bandwidth of 6.36 GHz (3.19-9.55 GHz), an insertion loss (S_{11}) of 17 dB from 4.14-8.7 GHz, and the group delay varies between 0.2 ns and 0.25 ns within the passband. This shows a better performance than that shown in Fig. 2. The optimized values are: W_1=1.57, L_1=4.51, W_2=5.2, L_2=4.9, W_3=1.55, L_3=g=2.2, h_1=h_2=0.51, W_m=7 and L_m=21.62 (all in mm).

2.3. Ultra-Wideband Bandpass Filter with Double Notched Bands

A meander line slot was introduced to reduce the circuit area, as shown in Fig. 5(a). This design offers a narrow notched band while minimizing the overall circuit size, as it eliminates the need for additional notch-generating components. Fig. 5(b) demonstrates that the length Ls determines the location of the notches, when Ls values are 6 mm, 7 mm, 8 mm and 9 mm, the corresponding resonant frequencies are 9.4 GHz, 8.2 GHz, 7.2 GHz, and 6.5 GHz, respectively. Furthermore, the width of the notched band can be modified by altering the dimensions of the meander line slot Ws. As illustrated in Fig. 5(c), when values of Ws are 0.8 mm, 1.0 mm and 1.2 mm, the 3-dB bandwidth of the notches measure 0.62 GHz, 1.06 GHz, and 1.94 GHz respectively, with a light shift in the frequencies. Therefore, by carefully modifying the meander-slot dimensions, it is feasible to generate adjustable notched bands with the desired bandwidth at the desired frequencies.

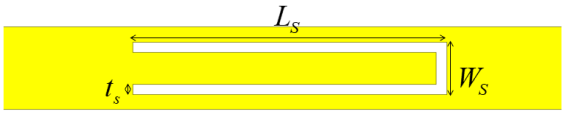

(a)

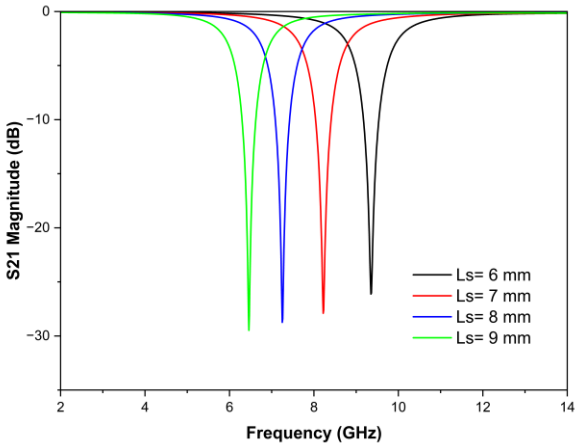

(b)

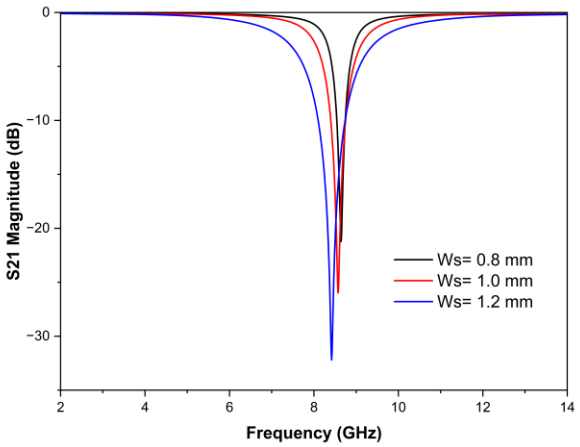

(c)

Figure 5. Meander slot analysis: (a) implementation of meander slot on 50 Ω microstrip line (b) Effect of length Ls when Ws = 1 mm (c) Effect of width Ws when Ls=6.8 mm.

The dimensions and location of the meander slots in the upper and bottom layers of the proposed ultra-wideband bandpass filter (UWB BPF) is shown in Fig. 6. This filter incorporates dual-notched bands with meander line slots positioned in the upper layer of the first patch from the input, and in the lower layer to the patch next to the output of the bandpass filter. These meander line slots create two narrow notched bands that eliminate undesired radio signals, whereas the UWB BPF generates a broad pass band with steep rolloffs at both the lower and upper cutoff frequencies. Folded meander slots were implemented on the patch at both the input and the output. To achieve sharp notches at 6.0 GHz and 7.6 GHz, the parameter values were selected as follows: Ws1=Ws4=Ws5=1 mm, Ws2=Ws6=0.8 mm, ts=0.2 mm and Ls=4mm, by maintaining other values unchanged.

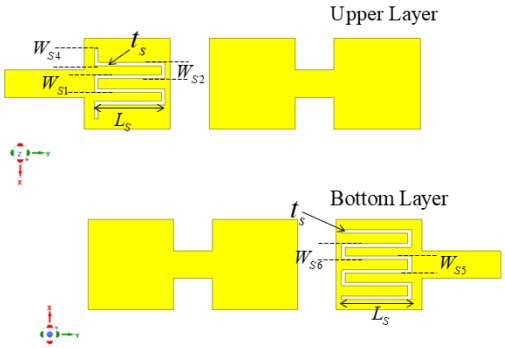

Figure 6. Upper and bottom layers of the proposed dual-notch bandpass filter.

3. Implementation and Results Analysis

This study utilized Rogers RT/duroid RO5880 high-frequency laminates as substrates, featuring a relative permittivity (εr) of 2.2, loss tangent of 0.0009, and thickness of 0.51 mm. The two layers were combined to create a multilayered filter. After optimizing the design parameters using HFSS software, a prototype of the filter circuit was constructed using multilayer PCB technology. The performance of this prototype was then assessed using an R&S ZVA vector network analyzer.

A photograph of the constructed filter is shown in Fig. 7, and Fig. 8 presents the simulated and measured S-parameters results. Notches occur at 6.0 GHz and 7.6 GHz, with attenuations of 19.89 dB (S21=19.89 dB) and 19.05 dB (S21=19.05 dB), respectively. The 3 dB relative bandwidths are 5.58% and 3.91%, respectively, demonstrating the sharpness of the notches. The in-band group delay is 0.3 ns, except at the notches. The measurements and simulations within the passband were aligned as closely as possible. However, the first notch experienced a shift from 6.0 GHz to 5.9 GHz, attributed to the fabrication errors of the meander slot on the bottom layer. The overall dimensions of the filter are 23.6 mm × 7 mm x 1.02 mm.

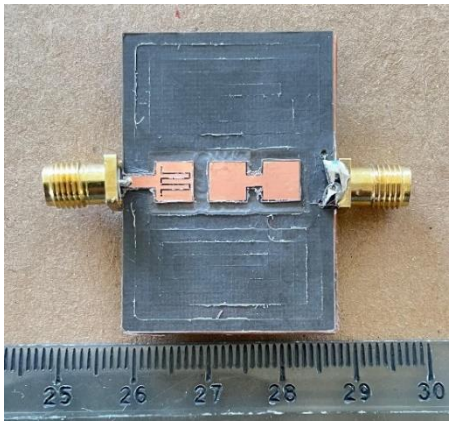

(a)

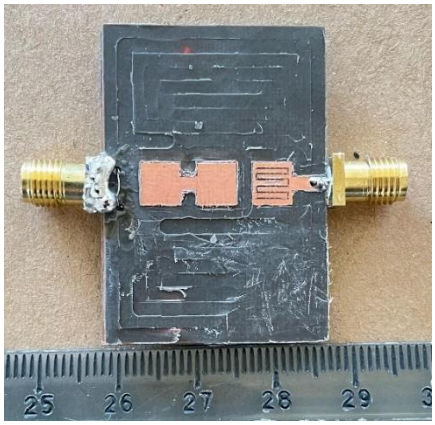

(b)

Figure 7. Photograph of the fabricated filter (a) upper layer
(b) bottom layer

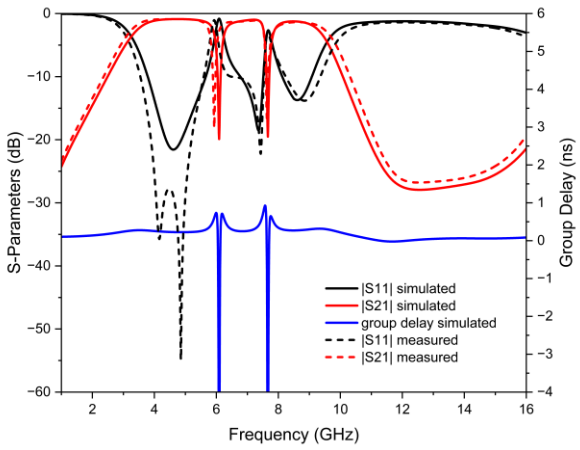

Figure 8. Simulated and measured results of dual-notched filter

As illustrated in Table 1, the analysis results demonstrate that the proposed filter achieves a fractional bandwidth exceeding 90%, with insertion losses consistently remaining below 1.3 dB across the passband. Additionally, it features two sharp notches and a compact size of 23.6 mm x 7.0 mm x 1.02 mm, thereby outperforming other designs referenced in the table.

Table 1. Comparison table with previous multilayered bandpass filters

Ref.	Filter technology	3 dB BW (GHz)	IL (dB) / RL (dB) in the passband	NF (GHz) / Att. (dB)	Size (mm x mm) / thickness (mm)
[19]	MPCB	1.5 - 9	<2 / >15	5.8 / 35	26.7 x 15 / 1.02
[23]	LCP	3.05 – 10.65	0.61 / >10	5.55 / 17.8	19.7 x 11.3 / 0.5
[24]	LTCC	3.1 – 12.4	0.5 / 14	5.8 / 20	7 x 8 / 0.55
[25]	LTCC	3 – 10.7	<1 / >10	5.2 / 15	6.0 x 6.0 / 1.92
This	**MPCB**	**3.18 – 9.79**	**<1.3 / >11**	**6.0, 7.6 / >19**	**23.6 x 7.0 / 1.02**

Ref: reference, BW: bandwidth, IL: insertion loss, RL: return loss, NF: notch frequency, Att: attenuation

The effective suppression of interference at notched frequencies demonstrates the ability of the filter to

improve the selectivity and maintain signal integrity in crowded spectral environments. This compact design, along with its adjustable notch characteristics, offers a flexible solution for addressing the challenges posed by unwanted signals in ultra-wideband applications.

4. Conclusion

This innovative dual-notched, multilayer, broadside-coupled UWB bandpass filter addresses the interference challenges in ultra-wideband systems through its distinctive configuration, which incorporates folded meander slots and a CPW-rectangular patch resonator. The filter exhibits exceptional selectivity and strong interference mitigation against WLAN and X-band satellite signals by employing notched bands at 6.0 GHz and 7.6 GHz. A compact and efficient design is achieved using a multilayer structure and broadside coupling without sacrificing performance, as evidenced by the close correlation between the simulated and experimental results. The compact size and adaptability of the filter make it an excellent candidate for contemporary UWB wireless communication systems that require space-efficient, high-performance filters. Subsequent research could explore additional notched bands to meet evolving interference requirements across various communication environments.

Acknowledgment

The financial support from the African Union (AU) through Pan-African University is gratefully acknowledged. This funding was instrumental to bringing the project to a successful conclusion.

References

[1] A. Alarifi *et al.*, "Ultra wideband indoor positioning technologies: Analysis and recent advances," *Sensors (Switzerland)*, vol. 16, no. 5, pp. 1–36, 2016, doi: 10.3390/s16050707.

[2] Z. C. Hao and J. S. Hong, "Multilayer interdigital ultra-wideband filter," *IEEE MTT-S Int. Microw. Symp. Dig.*, pp. 1–4, 2011, doi: 10.1109/MWSYM.2011.5972595.

[3] H. Shaman, S. Almorqi, and A. Alamoudi, "Ultra-wideband (UWB) Bandpass Filter with Cascaded Lowpass Filter on Multilayer Liquid-Crystal Polymer (LCP) Substrate," *IETE J. Res.*, vol. 62, no. 1, pp. 63–67, 2016, doi: 10.1080/03772063.2015.1082448.

[4] F. Huang, K. Aliqab, J. Wang, J. Hong, and W. Wu, "Self-Packaged Ultra-Wideband Balanced Bandpass Filter Using Multilayer Liquid Crystal Polymer Circuit Technology," *2019 IEEE MTT-S Int. Wirel. Symp. IWS 2019 - Proc.*, pp. 1–3, 2019, doi: 10.1109/IEEE-IWS.2019.8803897.

[5] K. Aliqab, "Wideband Notched Balun with Bandpass Filtering Characteristic Using Liquid Crystal Polymer Technology," *Proc. World Congr. Electr. Eng. Comput. Syst. Sci.*, pp. 2–8, 2023, doi: 10.11159/eee23.114.

[6] F. Huang, K. Aliqab, M. Hu, and Y. J. Zhu, "Design of a New Balanced Filter with Wideband DM Harmonic Elimination Based on Multilayer LCP Lamination Technology," *IEEE MTT-S Int. Microw. Work. Ser. Adv. Mater. Process. RF THz Appl. IMWS-AMP 2022 - Proc.*, pp. 1–3, 2022, doi: 10.1109/IMWS-AMP54652.2022.10106998.

[7] T. Kaneko and Y. Horii, "LTCC-based multi-layered UWB bandpass filter with broadside coupled E-shaped electrodes for significant size reduction and improvement of out-of-band response," *Asia-Pacific Microw. Conf. Proceedings, APMC*, no. d, pp. 773–775, 2012, doi: 10.1109/APMC.2012.6421731.

[8] K. Ruman, A. Pietrikova, I. Vehec, and P. Galajda, "Design of microstrip band pass filter based on LTCC for UWB sensor system," *Proc. Int. Spring Semin. Electron. Technol.*, pp. 237–241, 2013, doi: 10.1109/ISSE.2013.6648249.

[9] X. Dai, X. Y. Zhang, H. L. Kao, B. H. Wei, J. X. Xu, and X. Li, "LTCC bandpass filter with wide stopband based on electric and magnetic coupling cancellation," *IEEE Trans. Components, Packag. Manuf. Technol.*, vol. 4, no. 10, pp. 1705–1713, 2014, doi: 10.1109/TCPMT.2014.2346240.

[10] J. X. Chen, Y. Zhan, and Q. Xue, "Novel LTCC distributed-element wideband bandpass filter based on the dual-mode stepped-impedance resonator," *IEEE Trans. Components, Packag. Manuf. Technol.*, vol. 5, no. 3, pp. 372–380, 2015, doi: 10.1109/TCPMT.2015.2401023.

[11] W. Tang, R. Xu, and L. Zhao, "A Miniaturized Bandpass Filter Based on LTCC," *2023 Int. Conf. Microw. Millim. Wave Technol. ICMMT 2023 - Proc.*, vol. 2, pp. 1–3, 2023, doi: 10.1109/ICMMT58241.2023.10276589.

[12] L. Yang *et al.*, "Novel Multilayered Ultra-Broadband Bandpass Filters on High-Impedance Slotline Resonators," *IEEE Trans. Microw. Theory Tech.*, vol. 67, no. 1, pp. 129–139, 2019, doi: 10.1109/TMTT.2018.2873330.

[13] H. Bouazzaoui, A. Manchec, R. Allanic, C. Quendo, B. Potelon, and F. Karpus, "Ultra-Wideband

Bandpass Filter Using Solder-Mask-Based Multilayer Technology," *2019 49th Eur. Microw. Conf. EuMC 2019*, pp. 192–195, 2019, doi: 10.23919/EuMC.2019.8910764.

[14] J. Qiang, F. Xu, L. Yang, and J. Zhan, "Enhanced Performance of Multilayer Bandpass Filter Using Slow-Wave Empty Substrate- Integrated Waveguide (SW-ESIW)," *IEEE Microw. Wirel. Components Lett.*, vol. 31, no. 12, pp. 1279–1282, 2021, doi: 10.1109/LMWC.2021.3110107.

[15] E. Fathi, F. Setoudeh, and M. B. Tavakoli, "Design and fabrication of a novel multilayer bandpass filter with high-order harmonics suppression using parallel coupled microstrip filter," *ETRI J.*, vol. 44, no. 2, pp. 260–273, 2022, doi: 10.4218/etrij.2020-0330.

[16] C. Li, Z. H. Ma, J. X. Chen, M. N. Wang, and J. M. Huang, "Design of a Compact Ultra-Wideband Microstrip Bandpass Filter," *Electron.*, vol. 12, no. 7, pp. 1–14, 2023, doi: 10.3390/electronics12071728.

[17] Y. Zhan, Y. Wu, K. Ma, and K. S. Yeo, "Miniaturized Multiband Substrate-Integrated Waveguide Bandpass Filters with Multi-Layer Configuration and High In-Band Isolation," *Electronics*, vol. 13, no. 3834, 2024, doi: 10.3390/electronics13193834.

[18] S. K. Hashemi, "Ultra small ultra-wideband bandpass filter using broadside coupled S-shape striplines with built-in tunable notched band," *Proc. - IEEE Int. Conf. Ultra-Wideband*, pp. 54–57, 2011, doi: 10.1109/ICUWB.2011.6058906.

[19] X. C. Ji, W. S. Ji, L. Y. Feng, Y. Y. Tong, and Z. Y. Zhang, "Design of a novel multi-layer wideband bandpass filter with a notched band," *Prog. Electromagn. Res. Lett.*, vol. 82, no. January, pp. 9–16, 2019, doi: 10.2528/PIERL18121101.

[20] S. K. Hashemi, "Notch Filters based on Multilayer Ring Resonators (MRR)," *Mediterr. Microw. Symp.*, vol. 2019-Octob, pp. 3–6, 2019, doi: 10.1109/MMS48040.2019.9157280.

[21] W. Ji, H. Du, Y. Tong, X. Ji, and L. Feng, "Filter Design Based on Multilayer Wide Side Coupling Structure," *Prog. Electromagn. Res. M*, vol. 128, no. March, pp. 31–39, 2024, doi: 10.2528/PIERM24030604.

[22] A. M. Abbosh, "Planar bandpass filters for ultra-wideband applications," *IEEE Trans. Microw. Theory Tech.*, vol. 55, no. 10, pp. 2262–2269, 2007, doi: 10.1109/TMTT.2007.906468.

[23] Z. C. Hao and J. S. Hong, "UWB bandpass filter with switchable notching band using multilayer LCP technology," *Eur. Microw. Week 2010, EuMW2010 Connect. World, Conf. Proc. - Eur. Microw. Conf. EuMC 2010*, pp. 17–20, 2010, doi: 10.23919/EUMC.2010.5615955.

[24] B. Fu, X. Wei, J. Liao, and X. Zhang, "A notched UWB filter with LTCC technology," *Proc. 2012 Int. Work. Microw. Millim. Wave Circuits Syst. Technol. MMWCST 2012*, pp. 389–392, 2012, doi: 10.1109/MMWCST.2012.6238144.

[25] C.-X. Zhou, Y.-X. Guo, L.-S. Wu, W. Wu, and Q. Xiao, "Notched Ultra-Wideband Filter based on Stepped-Impedance T-Shaped Resontor in Low Temperature Cofired Ceramic," *IEEE Int. Wirel. Symp.*, vol. 14, no. 4, 2014, doi: 10.1109/IEEE-IWS.2014.6864255.